

REPORT

CHROMATIN

RPA binds histone H3-H4 and functions in DNA replication-coupled nucleosome assembly

Shaofeng Liu,^{1,2*} Zhiyun Xu,^{1*} He Leng,^{1,3*} Pu Zheng,¹ Jiayi Yang,¹ Kaifu Chen,⁴ Jianxun Feng,¹ Qing Li^{1†}

DNA replication-coupled nucleosome assembly is essential to maintain genome integrity and retain epigenetic information. Multiple involved histone chaperones have been identified, but how nucleosome assembly is coupled to DNA replication remains elusive. Here we show that replication protein A (RPA), an essential replisome component that binds single-stranded DNA, has a role in replication-coupled nucleosome assembly. RPA directly binds free H3-H4. Assays using a synthetic sequence that mimics freshly unwound single-stranded DNA at replication fork showed that RPA promotes DNA-(H3-H4) complex formation immediately adjacent to double-stranded DNA. Further, an RPA mutant defective in H3-H4 binding exhibited attenuated nucleosome assembly on nascent chromatin. Thus, we propose that RPA functions as a platform for targeting histone deposition to replication fork, through which RPA couples nucleosome assembly with ongoing DNA replication.

Nucleosome assembly during S phase is tightly coupled to DNA replication (1). The initial step of replication-coupled (RC) nucleosome assembly is the deposition of histone H3-H4 onto replicating DNA, which is followed by the rapid deposition of histone H2A-H2B (2, 3). Deposition of new histone H3-H4 requires the action of histone chaperones (4). Replication protein A (RPA), a complex that in yeast is composed of the Rfa1, Rfa2, and Rfa3 subunits, binds single-stranded DNA (ssDNA) at replication forks after double-stranded DNA (dsDNA) is unwound by the replicative helicase minichromosome maintenance (MCM), facilitates the movement of the replisome, and functions as a “unique harbor and binding platform” during DNA transactions (5–8). We studied the potential roles of RPA in RC nucleosome assembly.

We first analyzed whether RPA interacts with histone chaperones involved in RC nucleosome assembly, including chromatin assembly factor-1 (CAF-1) (9), anti-silencing function 1 (Asf1) (10), regulator of Ty1 transposition 106 (Rtt106) (11), and facilitates chromatin transactions (FACT) (12, 13). RPA subunit Rfa2 bound CAF-1, FACT, and Rtt106, but did not bind Asf1 (Fig. 1A and fig.

S1A). CAF-1 is recruited to DNA replication forks, in part, through its interaction with proliferating cell nuclear antigen (PCNA) (14–16). The RPA-CAF-1 interaction was unaffected in PCNA mutant (*pol30-879*) cells defective for the PCNA-CAF-1 interaction (16) (Fig. 1B), indicating that the RPA-CAF-1 interaction occurs independently of the PCNA-CAF-1 interaction. Moreover, histone H3-H4 promoted the interaction between RPA with each histone chaperone in vitro (fig. S1, B to E).

RPA copurifies with both histones H3 and H4 (17). We confirmed this interaction and showed that the RPA-H3-H4 interaction was not mediated by DNA (Fig. 1C). In vitro binding assays demonstrated that recombinant RPA directly binds free H3-H4, but not (mono)nucleosomal histone H3-H4 and free histone H2A-H2B dimers (Fig. 1D and fig. S2, A to C). The efficiency of H3-H4 binding increased for ssDNA-bound RPA, indicating that the RPA-H3-H4 interaction likely occurs on chromatin (Fig. 1E). In parallel assays for Asf1, ssDNA did not affect the efficiency of Asf1-H3-H4 binding (Fig. 1E). Domain mapping studies revealed that Rfa1, and specifically its oligonucleotide/oligosaccharide-binding fold domain at the N terminus (OB-N), was likely the major contributing site of the RPA-histone interaction (fig. S2, D to H).

Rfa1 immunoprecipitation (IP) analysis in cells showed that the RPA-H3-H4 interaction peaked during S phase (Fig. 1F and fig. S2I). We detected modifications of newly synthesized histones that were copurified with RPA, including acetylation of lysine 56 of H3 (H3K56Ac) (18) and acetylation of lysines 5 and 12 of H4 (H4K5,12Ac) (19) (Fig. 1, C and F to H), indicating that some portion of the RPA-bound H3-H4 population includes newly

synthesized histone H3-H4. H3K56Ac facilitates the interaction between H3-H4 and chaperones CAF-1 and Rtt106, thereby promoting RC nucleosome assembly (20). The RPA-H3-H4 interaction was reduced in mutant cells lacking one or more regulators of RC nucleosome assembly, including H3K56Ac (mutants *asf1Δ* and *rtt109Δ*) (Fig. 1G) and chaperones (mutant *cac1Δrtt106Δ*) (Fig. 1H). Deletion of *HIR1* (*hir1Δ*), a histone chaperone involved in replication-independent nucleosome assembly, did not affect this interaction (Fig. 1H). Our IP and in vitro binding assays demonstrated that RPA binds histone H3-H4 and showed that this RPA-H3-H4 interaction occurs concurrently with RC nucleosome assembly.

We used electrophoretic mobility shift assays (EMSAs) to examine the importance of the RPA-H3-H4 interaction in the formation of DNA-histone complexes. To mimic freshly unwound ssDNA at the replication fork, we designed a fluorescently labeled substrate that consisted of a 149-base pair (bp) Widom601-dsDNA fragment with a 75-nucleotide (nt) ssDNA overhang (ss-dsDNA). Two DNA-(H3-H4) species migrating at the positions characteristic of tetrasomes or disomes were detected when histone H3-H4 tetramers were incubated with the control dsDNA (Fig. 2A, lane 14, and fig. S3, lane 2) (21), an unmodified 149-bp Widom601-dsDNA [dsDNA(149)] (22). A shifted band confirmed that DNA-(H3-H4) complexes formed with the ss-dsDNA substrate (Fig. 2A, lane 2, and fig. S3, lane 9). By itself, RPA bound to ss-dsDNA (RPA-DNA) but had very low affinity for dsDNA(149), supporting the idea that RPA binds the ssDNA region of the ss-dsDNA substrate (Fig. 2A, lanes 3 and 15, and fig. S3, lanes 10 and 3). A large complex formed on the ss-dsDNA substrate and did so in an RPA concentration-dependent manner (Fig. 2A, lanes 4 to 7, and fig. S3, lanes 11 to 14). Western blot analysis of the same gel revealed that both H3 and RPA were located at the same position as the shifted band, indicating that the large complex contains RPA, histones H3-H4, and DNA [RPA-DNA-(H3-H4)]. Additionally, the density of the ss-dsDNA band decreased in a manner concomitant with RPA-DNA-(H3-H4) formation, indicating that RPA promotes the assembly of histones with DNA. RPA had no apparent effect on the formation of tetrasome or disome species on dsDNA(149) substrates (Fig. 2A, lanes 15 to 19, and fig. S3, lanes 3 to 7).

To discern whether H3-H4 assembled at the ssDNA or the dsDNA region of the ss-dsDNA substrate, we digested the EMSA reaction products with the restriction endonuclease Hha I, which cuts in the middle of the dsDNA region. Without H3-H4 and irrespective of RPA, Hha I treatment yielded two DNA fragments (Fig. 2B, lanes 2 and 6). With only H3-H4, DNA-(H3-H4) complex formation prevented Hha I digestion, suggesting that the Hha I site was occupied by H3-H4 (Fig. 2B, compare lane 4 with lane 3). The RPA-DNA-(H3-H4) complex also prevented Hha I digestion (Fig. 2B, compare lane 8 with lane 7). Moreover, N-terminally truncated RPA complex (ΔN) exhibited a marked reduction in RPA-DNA-(H3-H4) formation (Fig. 2C). These in vitro results

¹State Key Laboratory of Protein and Plant Gene Research, School of Life Sciences and Peking-Tsinghua Center for Life Sciences, Peking University, Beijing 100871, China. ²Peking University-Tsinghua University-National Institute of Biological Sciences Joint Graduate Program, School of Life Sciences, Tsinghua University, Beijing 100084, China.

³Academy for Advanced Interdisciplinary Studies, Peking University, Beijing 100871, China. ⁴Center for Cardiovascular Regeneration, DeBakey Heart and Vascular Center, Houston Methodist, Houston, TX 77030, USA.

*These authors contributed equally to this work.

†Corresponding author. Email: li.qing@pku.edu.cn

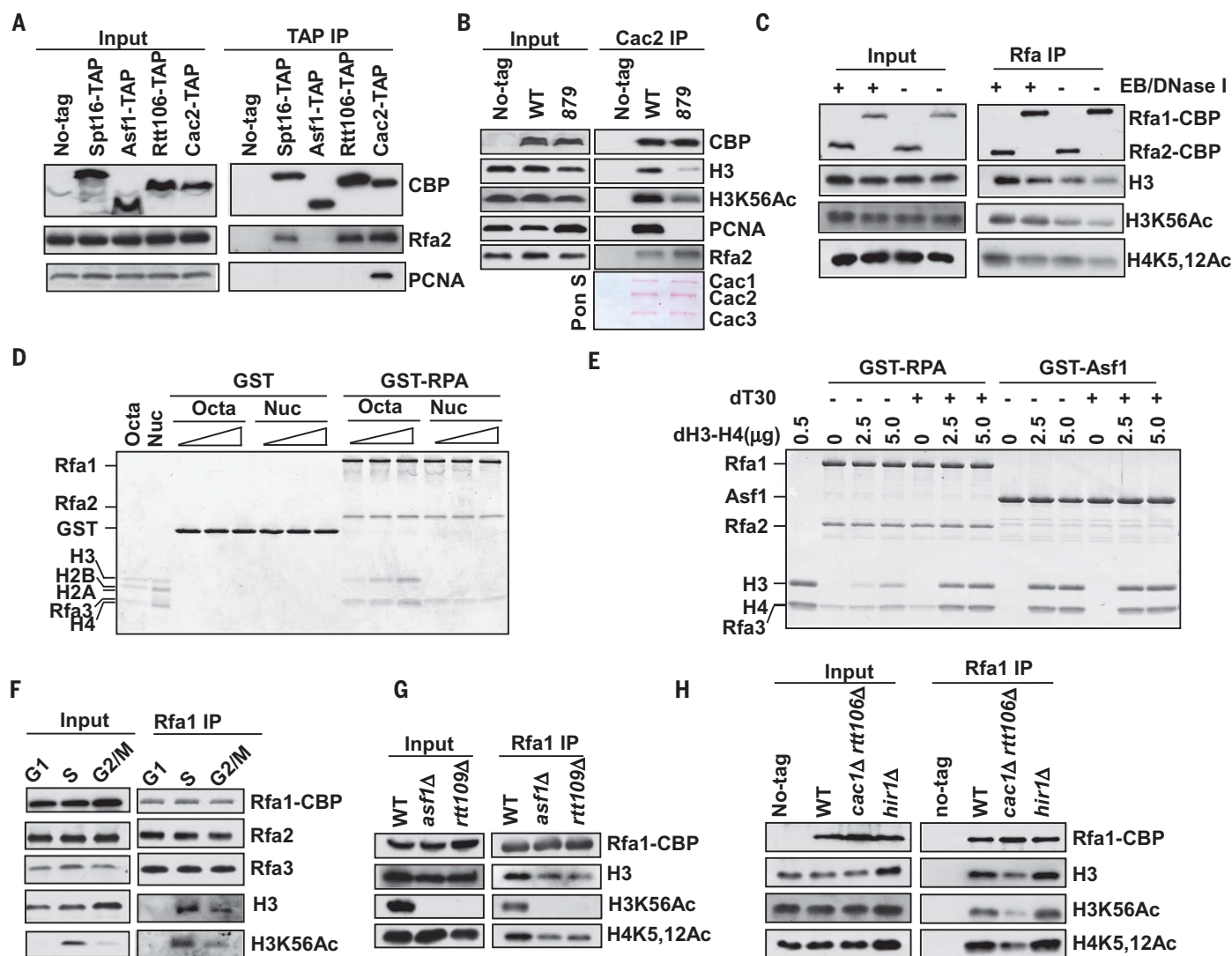


Fig. 1. The RPA complex interacts with histone chaperones and histone H3-H4. (A) Tandem affinity purification (TAP)-tagged histone chaperones Spt16 (subunit of FACT complex), Asf1, Rtt106, and Cac2 (subunit of CAF-1 complex) were purified from yeast cells. Copurified proteins (IP) and proteins in cell extracts (input) were immunoblotted with the indicated antibodies. CBP, calmodulin-binding peptide; no-tag, the control strain lacking TAP-tagged proteins. (B) Cac2-TAP was purified from wild-type (WT) and PCNA mutant (*pol30-879*) cells. The purified CAF-1 complex was visualized by Ponceau S staining (Pon S). CAF-1 complex consists of subunits Cac1, Cac2, and Cac3 (C) Rfa1-TAP and Rfa2-TAP were each purified with or without deoxyribonuclease I (DNase I) and ethidium bromide (EB). (D) Recombinant glutathione S-transferase

(GST)-RPA complex and GST proteins were used to immunoprecipitate (pull down) recombinant core histone octamers (octa) or (mono)nucleosomal histones (nuc), and bound proteins were analyzed by Coomassie Brilliant Blue (CBB) staining. (E) Recombinant GST-RPA complex and GST-Asf1 proteins were used to pull down recombinant *Drosophila* histone H3-H4 (dH3-H4) tetramers in the presence or absence of a 30-nt oligonucleotide-deoxythymine (dT) (dT30). Bound proteins were analyzed by CBB staining. (F) Analysis of Rfa1-TAP associated histone H3-H4 from cells at the G₁ (0 min), S (40 min), and G₂/M (80 min) phases of the cell cycle. DNA content was determined by flow cytometric analysis (fig. S2I). (G and H) Analysis of Rfa1-TAP associated proteins from WT cells and *asf1Δ*, *rtt109Δ*, *cac1Δrtt106Δ*, and *hir1Δ* mutant cells.

support a model in which RPA residing on ssDNA binds H3-H4 to promote the assembly of H3-H4 onto immediately adjacent dsDNA.

We found a mutant allele (*rfa1-A88P*) with reduced H3-H4 binding (Fig. 3A and fig. S4, A and B). In the *rfa1-A88P* mutant cells, the interaction of RPA with histone chaperones CAF-1, FACT, and Rtt106 was compromised (fig. S4, C to E), likely because histone H3-H4 bridged this interaction (fig. S1, B to E). Rfa1-A88P mutant proteins bound to fired replication origins like wild-type RPA (Fig. 3, B and C). This mutant allele interacted genetically with mutations at factors in RC nucleosome assembly (fig. S4F) (12). Together,

these results suggest a potential role for RPA in RC nucleosome assembly. Therefore, we used multiple assays to analyze the effect of the *rfa1-A88P* mutation on H3 deposition during DNA replication (20). First, in *rfa1-A88P* mutant cells, we observed an apparent reduction of H3K56Ac, which is deposited onto chromatin concurrently with DNA synthesis (20), at replicating DNA regions in cells synchronized at early S phase by hydroxyurea (HU) (Fig. 3D and fig. S5). No obvious changes in total H3K56Ac and RPA levels or in HU-synchronization were observed in mutant cells (fig. S6), and the HU-synchronization condition had no effect on the viability of *rfa1-*

A88P mutant cells (fig. S7). Second, a similar H3K56Ac deposition defect was observed in *rfa1-A88P* mutant cells during normal cell cycle progression (Fig. 3E and fig. S8). Third, we observed that Rfa1-A88P mutant proteins exhibited reduced ability to assemble H3-H4 onto ss-dsDNA substrate compared with wild-type RPA proteins in vitro (fig. S9). Thus, the RPA-H3-H4 interaction influences the extent of new H3 deposition onto the replication fork.

To examine nucleosome formation on nascent chromatin, we used micrococcal nuclease (MNase) digestion to evaluate the chromatin accessibility of both bulk and nascent chromatin. We labeled

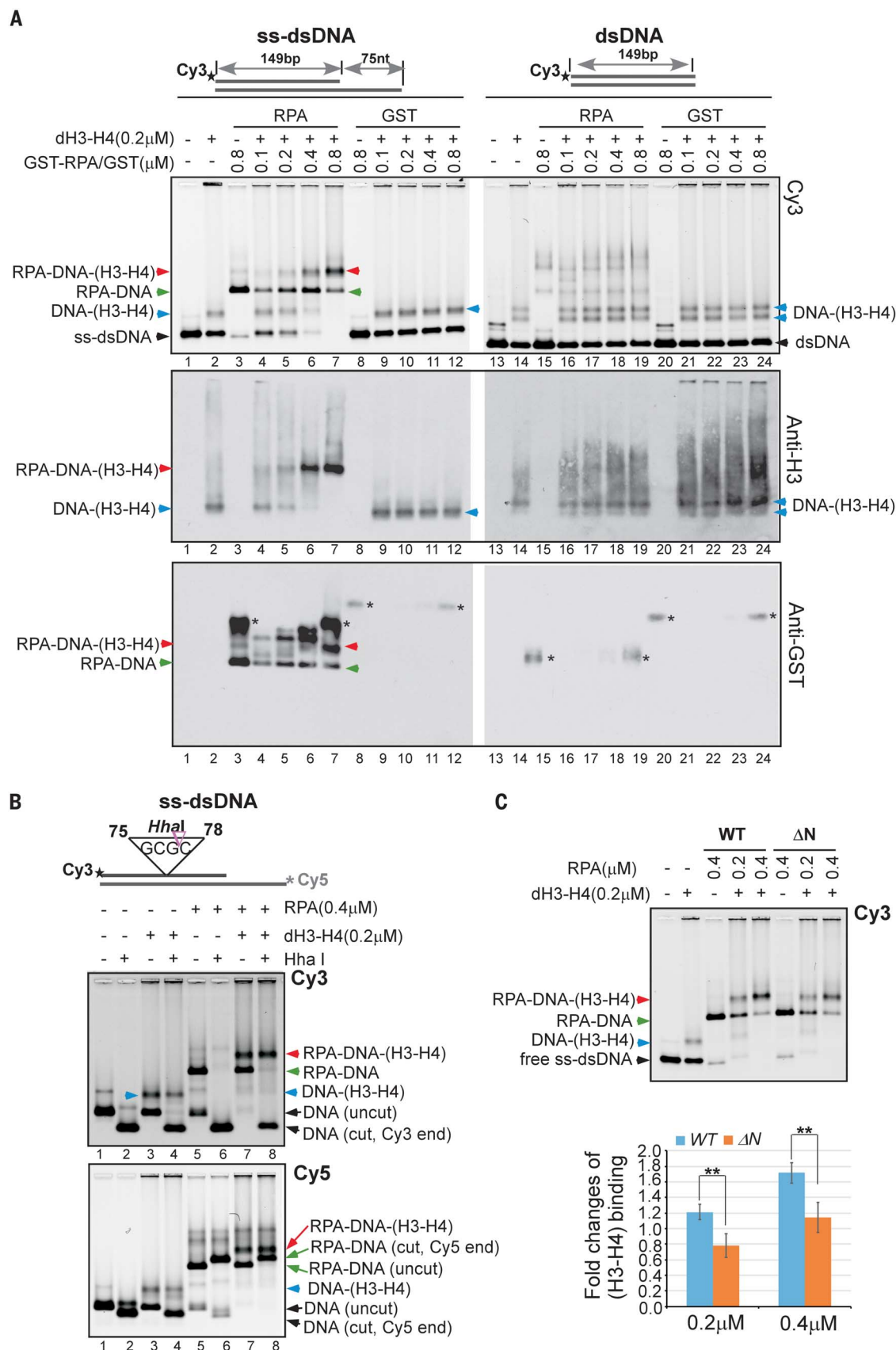


Fig. 2. RPA promotes assembly of H3-H4 onto dsDNA adjacent

protein substrates labeled with cyanine 3 dye (Cy3) at the dsDNA end were used for EMSA (top). GST-RPA complexes and control GST proteins were used for EMSA experiments using fluorescently labeled DNA substrates with or without dH3-H4. Free DNA and the protein-DNA complexes were detected by a Typhoon FLA 9500 imager (upper panel). Proteins from the same EMSA gel were transferred to a nitrocellulose membrane and immunoblotted with antibodies against H3 (anti-H3, middle panel) and GST (anti-GST, bottom panel). *, protein aggregates. **(B)** The same ss-dsDNA substrate was used as in **(A)** with additional labeling by cyanine 5 dye (Cy5) at the ssDNA end (top). A representative EMSA result showing complexes detected by Cy3 (upper panel) and Cy5 (bottom panel) with or without Hha I digestion (cut and uncut, respectively) of the reaction mixtures. Similar results were obtained from at least three independent experiments. **(C)** An experiment was performed using wild-type (WT) and N-terminally truncated (Δ N) RPA proteins as described in **(A)** (top). The quantification results were from four independent experiments (bottom). A paired Student's *t* test was used to calculate the *P* value (**0.001 < *P* value \leq 0.01).

nascent chromatin in S-phase cells with the thymidine analog 5-bromo-2'-deoxyuridine (BrdU) during DNA synthesis. Whereas bulk chromatin accessibility was not affected in *rfa1-A88P* mutant cells, nascent chromatin was more susceptible to MNase digestion, suggesting that nucleosome assembly at nascent chromatin is reduced in *rfa1-A88P* mutant cells (fig. S10). To quantify nucleosome formation on nascent chromatin at

the genome-wide level, we developed a method termed replication-intermediate nucleosome mapping (ReIN-Map) (Fig. 4A). As part of this method, nascent chromatin was also labeled with BrdU during DNA synthesis, and chromatin samples from HU-synchronized early S phase cells were divided and fragmented using either MNase or sonication treatment (input). These input samples were then subjected to IP with antibodies against

BrdU (BrdU-IP) to enrich nascent chromatin, followed by strand-specific sequencing. The nucleosome assembly-defective mutant *rtt109Δ* was used as a control (20). Nucleosome phase plots revealed that the nucleosome occupancy patterns around the transcription start sites (TSSs) and around the autonomously replicating sequences (ARS) consensus sequences (ACSS) were similar among wild-type, *rfa1-A88P*, and *rtt109Δ* cells at G₁ phase (Fig. 4B and figs. S11, A and C, and S12, A and C), indicating that the *rfa1-A88P* and *rtt109Δ* mutations did not affect the overall organization of nucleosomes on mature chromatin. Although nucleosome occupancy was similar among wild-type cells and *rfa1-A88P* and *rtt109Δ* mutant cells at TSSs (figs. S11B and S12, B and D), nucleosome occupancy in wild-type cells was reduced compared to mutant cells at ACSs, where BrdU is present at early S phase (Fig. 4C and fig. S11D). Moreover, the average BrdU density at ACSs in wild-type cells was higher than in mutant cells (Fig. 4E, figs. S13 and S14, and table S1). These results suggest that the reduced total nucleosome occupancy in wild-type cells is related to a relatively higher proportion of nascent nucleosomes, consistent with the idea that nascent chromatin is more susceptible to MNase digestion because the newly replicated chromatin surrounding ACSs is immature.

We then aligned the MNase-BrdU-IP enriched fragments to the *Saccharomyces cerevisiae* genome and observed properly occupied nucleosomes surrounding ACSs in wild-type early S phase cells. A substantial reduction in nucleosome occupancy surrounding ACSs was observed in *rfa1-A88P* and *rtt109Δ* mutant cells (Fig. 4D and fig. S15). This reduction potentially reflects both reduced DNA synthesis resulting from sonication-BrdU-IP-seq (Fig. 4E) and compromised nucleosome assembly itself. To evaluate nucleosome assembly defects in *rfa1-A88P* mutant cells during DNA synthesis, we normalized MNase-BrdU-IP-seq signals using sonication-BrdU-IP-seq signals to derive a ReIN score, which is the quotient of nascent nucleosome coverage based on the MNase-BrdU-IP-seq signal over the nascent DNA coverage represented by the sonication-BrdU-IP-seq signal. To reduce the potential overestimation of ReIN scores for bases with low sequencing coverage, raw genome counts for sonication-BrdU-IP-seq quantitation were simulated by smoothing based on an exponential model (Fig. 4E, right). The ReIN scores surrounding ACSs were reduced in mutant cells, and the degree of reduction in *rfa1-A88P* mutant cells was comparable to that of *rtt109Δ* mutant cells (Fig. 4F). Thus, nucleosome assembly on nascent chromatin is compromised by disruption of the RPA-H3-H4 interaction.

In this study, we suggest that RPA, an essential replisome component, provides a binding platform for histone H3-H4 and multiple histone H3-H4 chaperones, including CAF-1, Rtt106, and FACT. Our results support a model whereby RPA binds ssDNA and promotes the deposition of H3-H4 onto adjacent dsDNA, in part through its ability to bind H3-H4. We observed that deoxyribonuclease I (DNase I) and ethidium bromide

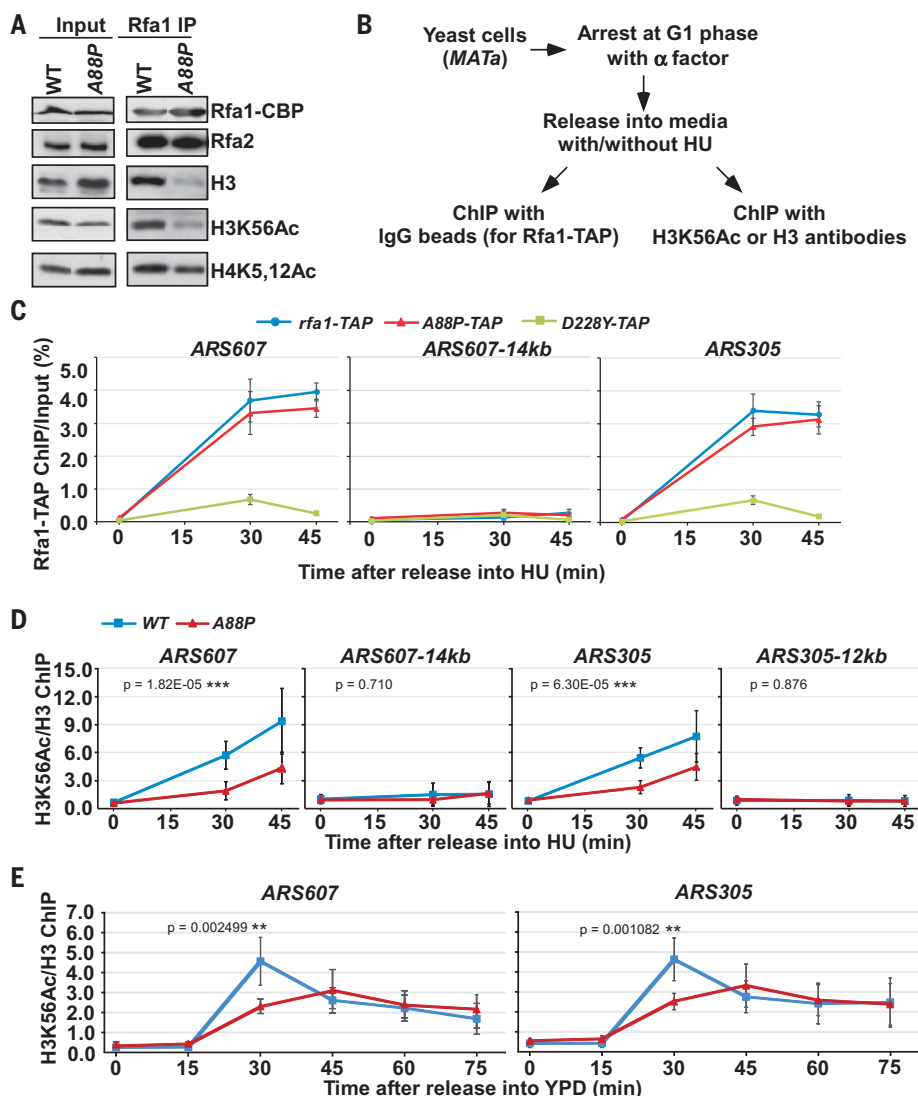
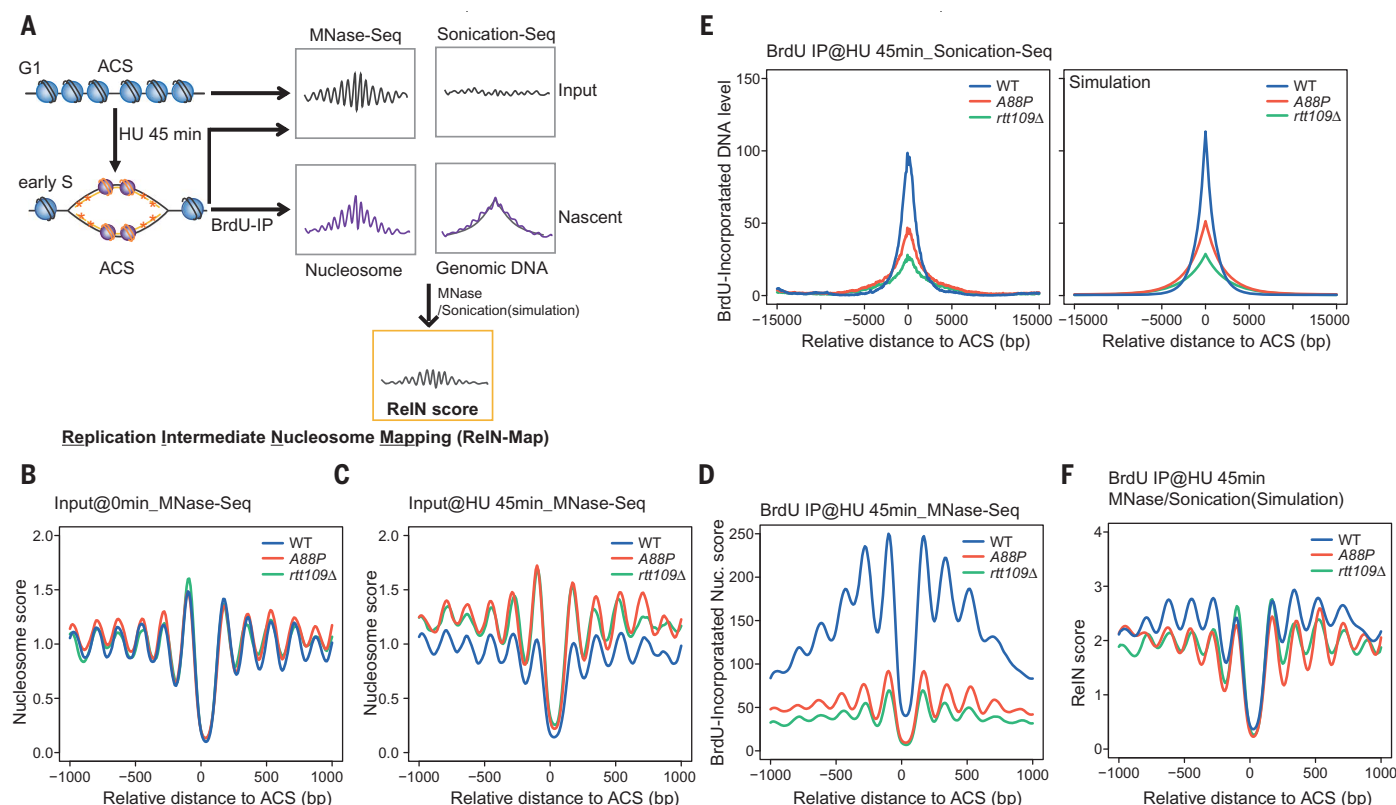


Fig. 3. Rfa1-A88P mutant exhibits reduced H3-H4 binding and defective deposition of H3K56Ac onto replicating DNA. (A) Analysis of the Rfa1-H3-H4 interaction by Rfa1-TAP purification in wild-type (WT) and *rfa1-A88P* mutant cells. (B) The experimental scheme for the Rfa1-TAP and H3K56Ac chromatin immunoprecipitation (ChIP) assays. IgG, immunoglobulin G; *MATa*, mating type a. (C) Rfa1-A88P binds fired replication origins like wild-type Rfa1. Error bars represent standard errors as calculated from three biological replicates. *D228Y*-TAP, *rfa1-D228Y* mutation; ARS305 and ARS607, fired early replication origins; ARS607-14kb, a corresponding nonreplicating distal region of ARS607. (D) H3K56Ac deposition is compromised in *rfa1-A88P* mutant cells at HU-synchronized early S phase. The ratio of H3K56Ac over H3 ChIP signal was calculated. ARS305-12kb, a corresponding nonreplicating distal region of ARS305. The mean and SD of three biological replicates are shown, with *P* values derived from two-way analysis of variance (ANOVA) (****P* value ≤ 0.001). (E) H3K56Ac deposition is compromised in *rfa1-A88P* mutant cells during normal S phase. The ratio of H3K56Ac over H3 ChIP signal was calculated. The mean and SD of three biological replicates are shown. The single-tailed nonparametric Wilcoxon test was performed as described in the supplementary methods (** $0.001 < P$ value ≤ 0.01). YPD, yeast extract-peptone-dextrose, a complete medium for yeast growth.



G₁ phase input samples was plotted relative to ACS. (C) Normalized nucleosome occupancy of early S phase input samples was plotted relative to ACS. (D) The average nucleosome occupancy surrounding BrdU-enriched ACS was calculated using sequenced reads from MNase-BrdU-IP samples. (E) The average BrdU density surrounding ACS was calculated with sequence reads from sonication-BrdU-IP samples (left). Simulations of nascent DNA patterns were generated by applying an exponential model (right). (F) The ReIN scores surrounding the ACS regions at early S phase of indicated strains are shown. The ReIN score is defined by the quotient of nascent nucleosome coverage based on the MNase-BrdU-IP-seq signal over the mathematically simulated nascent DNA coverage from the sonication-BrdU-IP-seq signal to reduce the potential overestimation of ReIN scores for bases with low sequencing coverage.

treatment of cell lysates resulted in a stronger RPA-H3-H4 interaction, implying that RPA may bind parental histones released from chromatin (22). Mcm2, a subunit of replicative helicase MCM, contains a motif that binds H3-H4 and is not required for DNA replication (23). MCM interacts with histone chaperones Asf1 and FACT (24), and the interactions between MCM and histone chaperones Asf1 and FACT have been proposed to facilitate nucleosome disassembly of parental H3-H4 following DNA replication (22, 24). RPA binds ssDNA immediately after the unwinding of dsDNA by MCM, prior to DNA synthesis (5). Given our finding that RPA functions in nucleosome assembly on nascent chromatin, we suggest that RPA provides a common binding platform for the coordination of histone deposition by multiple histone chaperones during RC nucleosome assembly.

REFERENCES AND NOTES

1. S. L. McKnight, O. L. Miller Jr., *Cell* **12**, 795–804 (1977).
2. G. Almouzni, D. J. Clark, M. Méchali, A. P. Wolffe, *Nucleic Acids Res.* **18**, 5767–5774 (1990).
3. S. Smith, B. Stillman, *EMBO J.* **10**, 971–980 (1991).
4. Z. A. Gurard-Levin, J.-P. Quivy, G. Almouzni, *Annu. Rev. Biochem.* **83**, 487–517 (2014).
5. M. S. Wold, *Annu. Rev. Biochem.* **66**, 61–92 (1997).
6. W. D. Heyer, M. R. Rao, L. F. Erdlie, T. J. Kelly, R. D. Kolodner, *EMBO J.* **9**, 2321–2329 (1990).
7. S. J. Brill, B. Stillman, *Nature* **342**, 92–95 (1989).
8. A. Maréchal, L. Zou, *Cell Res.* **25**, 9–23 (2015).
9. S. Smith, B. Stillman, *Cell* **58**, 15–25 (1989).
10. J. K. Tyler et al., *Nature* **402**, 555–560 (1999).
11. S. Huang et al., *Proc. Natl. Acad. Sci. U.S.A.* **102**, 13410–13415 (2005).
12. A. P. VanDemark et al., *Mol. Cell* **22**, 363–374 (2006).
13. J. Yang et al., *Cell Rep.* **14**, 1128–1141 (2016).
14. K. Shibahara, B. Stillman, *Cell* **96**, 575–585 (1999).
15. J. G. Moggs et al., *Mol. Cell. Biol.* **20**, 1206–1218 (2000).
16. Z. Zhang, K.-I. Shibahara, B. Stillman, *Nature* **408**, 221–225 (2000).
17. J. M. Gilmore et al., *Mol. Cell. Proteomics* **11**, 011544 (2012).
18. H. Masumoto, D. Hawke, R. Kobayashi, A. Verreault, *Nature* **436**, 294–298 (2005).
19. A. Ruiz-Carrillo, L. J. Wangh, V. G. Allfrey, *Science* **190**, 117–128 (1975).
20. Q. Li et al., *Cell* **134**, 244–255 (2008).
21. D. C. Donham 2nd, J. K. Scorgie, M. E. A. Churchill, *Nucleic Acids Res.* **39**, 5449–5458 (2011).
22. M. Foltman et al., *Cell Rep.* **3**, 892–904 (2013).
23. H. Huang et al., *Nat. Struct. Mol. Biol.* **22**, 618–626 (2015).
24. A. Groth et al., *Science* **318**, 1928–1931 (2007).

ACKNOWLEDGMENTS

We thank Z. Zhang, R. Burgess, K.-M. Chan, and H. Wu for critical reading of the manuscript. We thank M. Wold, O. Aparicio, R. Xu, G. Li, S. Brill, M. Grunstein, G. Camilloni, and J. Tyler for reagents and suggestions for experimental procedures. We thank the Biodynamic Optical Imaging Center (BIOPTIC) sequencing facility at Peking University for assistance with sequencing. This work was supported by National Natural Science Foundation of China (NSFC) grants (31322017 and 31370767). K.C. is supported, in part, by an NIH grant (HL100397). The high-throughput sequencing data sets have been deposited at the National Center for Biotechnology Information (NCBI) Gene Expression Omnibus (GEO) database (accession identifier GSE83648).

SUPPLEMENTARY MATERIALS

www.sciencemag.org/content/355/6323/415/suppl/DC1
Materials and Methods
Figs. S1 to S15
Tables S1 to S3
References (25–39)

16 July 2016; accepted 21 December 2016
10.1126/science.aah4712

RPA binds histone H3-H4 and functions in DNA replication–coupled nucleosome assembly

Shaofeng Liu, Zhiyun Xu, He Leng, Pu Zheng, Jiayi Yang, Kaifu Chen, Jianxun Feng and Qing Li

Science **355** (6323), 415-420.
DOI: 10.1126/science.aah4712

The platform for building new chromatin

Nucleosomes removed from DNA to facilitate its replication must be replaced quickly to protect the genome. The epigenetic information stored on the parental nucleosomes must also be preserved on the daughter DNA strands. The replication protein A complex (RPA) is a critical component of the DNA replication machinery. RPA binds single-stranded DNA. Liu *et al.* show that RPA bound to a single-stranded DNA replication fork mimic recruits and promotes the assembly of H3-H4 histone tetramers onto adjacent double-stranded DNA. It also recruits specific H3-H4 chaperones, which facilitate the assembly of new nucleosomes.

Science, this issue p. 415

ARTICLE TOOLS

<http://science.sciencemag.org/content/355/6323/415>

SUPPLEMENTARY MATERIALS

<http://science.sciencemag.org/content/suppl/2017/01/25/355.6323.415.DC1>

REFERENCES

This article cites 39 articles, 10 of which you can access for free
<http://science.sciencemag.org/content/355/6323/415#BIBL>

PERMISSIONS

<http://www.sciencemag.org/help/reprints-and-permissions>

Use of this article is subject to the [Terms of Service](#)